Reconstruction of the TeV Emission Morphology in the Cygnus X Region Using the Richardson–Lucy Algorithm

Guangwei Wang (USTC), Ruizhi Yang (USTC), Yang Su (PMO)

April 2026

Overview

Contents

1 Motivation

Non-parametric model

Limitations of model-based Likelihood Fitting

Model-based Likelihood Fitting works well simple parametric shapes (e.g., Gaussian) and in cases where the statistics are low.

However, at TeV energies:

- Extended sources dominate, a simple model may lose important morphological information and waste the available statistics.
- To get more information in complex regions with high statistics results in an unsustainable growth of model choice combinations.
- Poor gas velocity resolution and non-uniform CR distribution greatly degrade template-based fitting.

To gain more clues, we can use a non-parametric method that reconstructs the true flux distribution without strong model assumptions.

For example, directly fitting an image where flux of each pixel is a free parameter.

Method Comparison

A Model based Likelihood Fitting

Strong regularization — parametric model

Pros: Fewer parameters, stable convergence

Cons: Biased if model is wrong

B Non-parametric model or image-based likelihood fitting

Weaker regularization — pixelated signal grid

Pros: More flexible, model-independent, recover the true flux distribution if statistic is enough

Cons: Difficult to converge, overfitting

The Richardson–Lucy Algorithm

Richardson-Lucy Algorithm is mathematically equivalent to an iterative maximum-likelihood algorithm for Poisson signal. *(Richardson 1972, Lucy 1974)*

Key Guarantees

1. Likelihood value **increases** every iteration
2. Flux remains **non-negative**

Optimization For KM2A Data

Declination translation invariance (PSF, distance), hardware acceleration, ...

~10^5× measured speedup

Enabling 3D RL deconvolution with RA × Dec × Energy-dependent response

Iteration formula

$$f_j^{(k+1)} = f_j^{(k)} \frac{1}{\sum_n R_{nj}} \sum_i R_{ij} \frac{N_{on,i}}{\sum_l R_{il} f_l^{(k)} + N_{bkg,i}}$$

Notation

$f_j^{(k)}$: Flux at source pixel j at iteration k

$N_{on,i}$: Observed counts at observation pixel i

$N_{bkg,i}$: Background at observation pixel i

R_{ij} : Response matrix

Physical Interpretation:

$$\text{ratio}_i = \frac{N_{on,i}}{\sum_l R_{il} f_l^{(k)} + N_{bkg,i}} = \frac{\textit{Observed Counts}}{\textit{Predicted Counts}}$$

Ratio > 1 → signal is underestimated → boost
Ratio < 1 → signal is overestimated → reduce

For each pixel *j*, then compute a weighted adjustment factor:

$$f_j^{(k+1)} = w_j\, f_j^{(k)}, \qquad w_j = \frac{\sum_i R_{ij} \times \text{ratio}_\text{i}}{\sum_i R_{ij}}$$

Deconvolution image of Crab Nebula

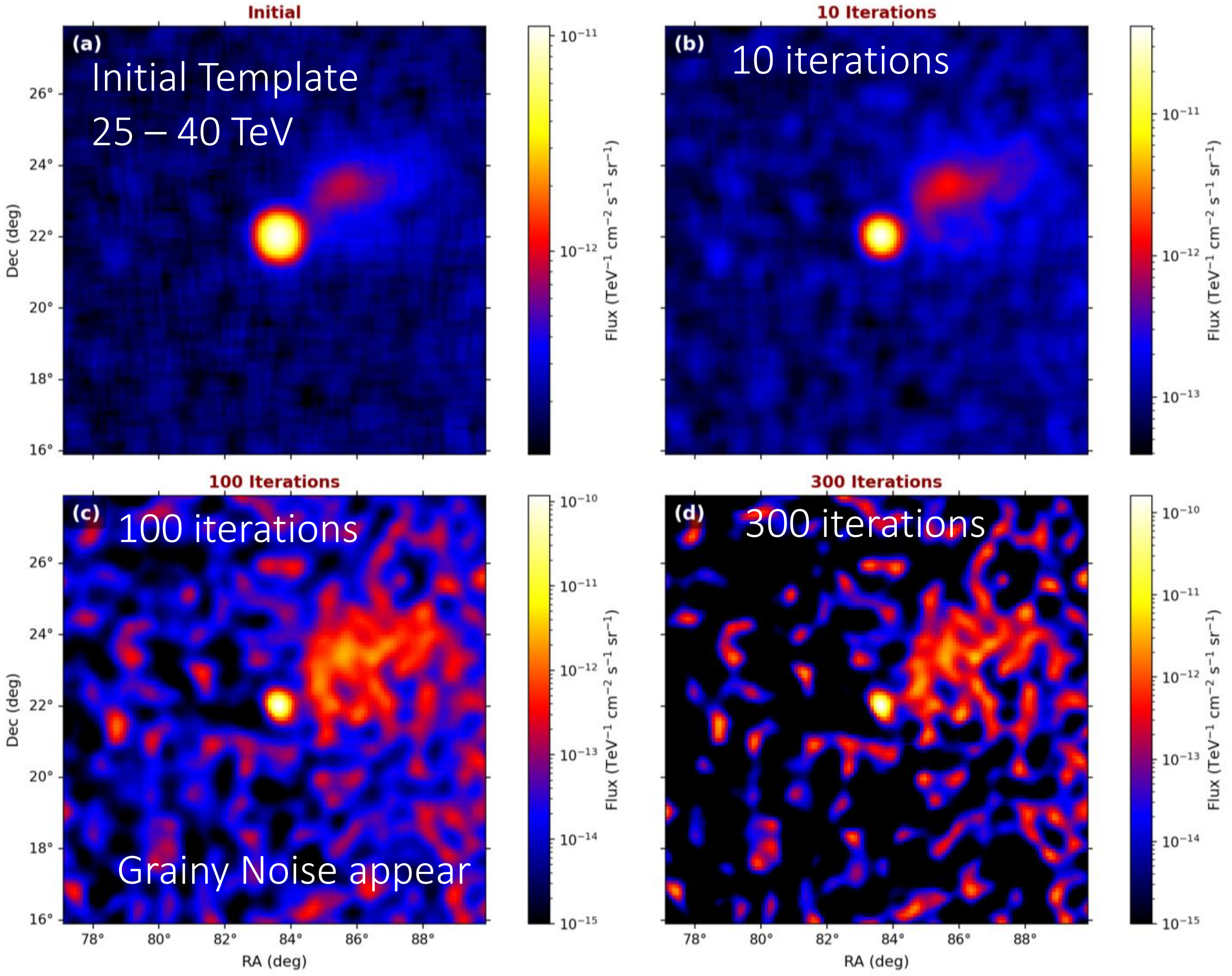

Data: all KM2A data to 20250731

Initail Template: Smoothed $\frac{N_{on} - N_{bkg}}{A_{eff} t}$

Image resolution improves, but noise occurs in later stages.

Deconvolution image of Crab Nebula

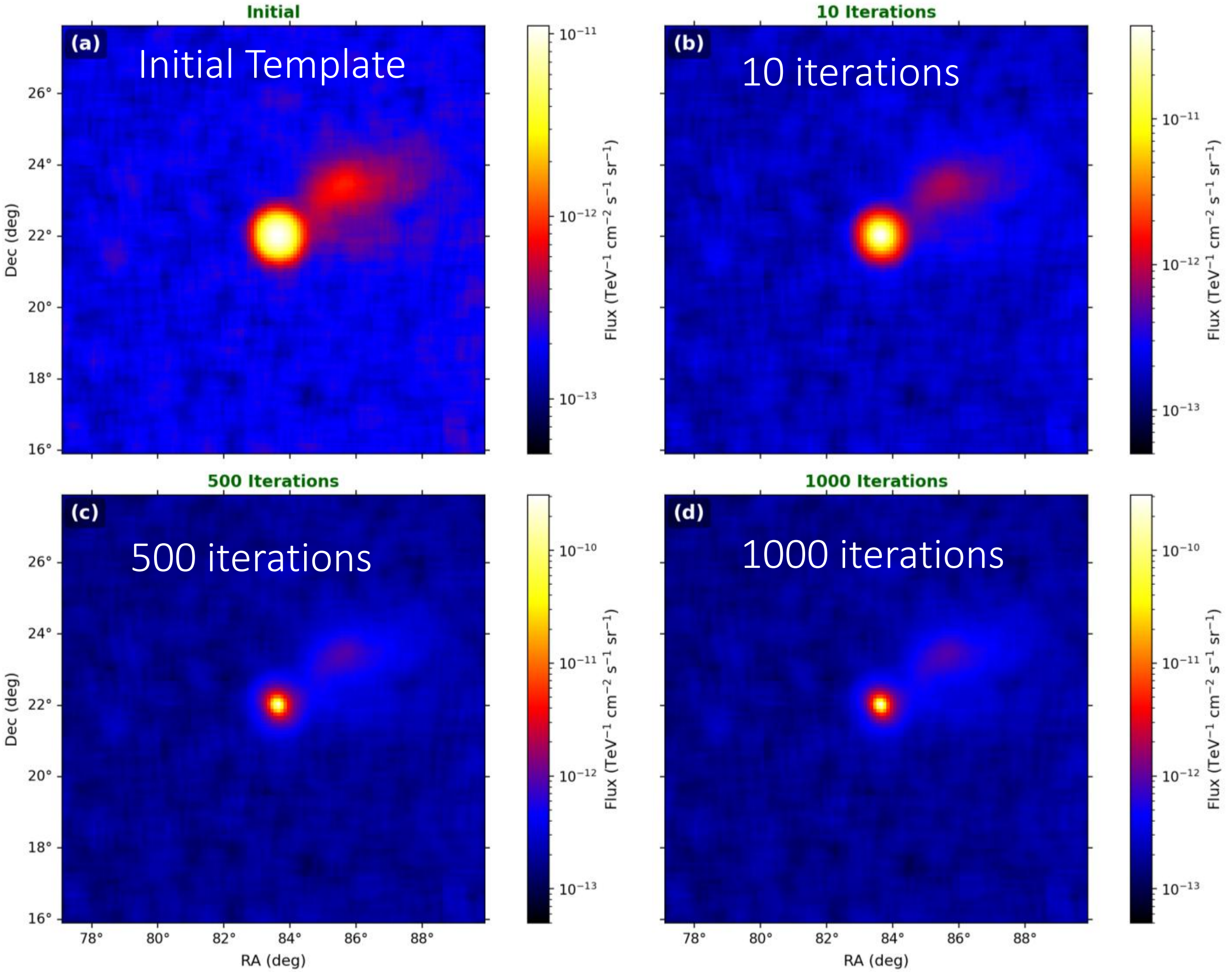

Damped RL

$$f_i^{new} = f_i \times \left[1 + tanh\left(\frac{|\Delta f_i|^2}{\left(n_\sigma \frac{N_{bkg,i}}{A_{eff} t}\right)^2}\right) \cdot \frac{\Delta f_i}{f_i}\right]$$

Δf_i: Update amount of the standard RL algorithm

A_{eff}: Effective area

t: Observation time

n_σ: Hyperparameter controlling the strength of noise suppression

Deconvolution image of Crab Nebula

More energy bands

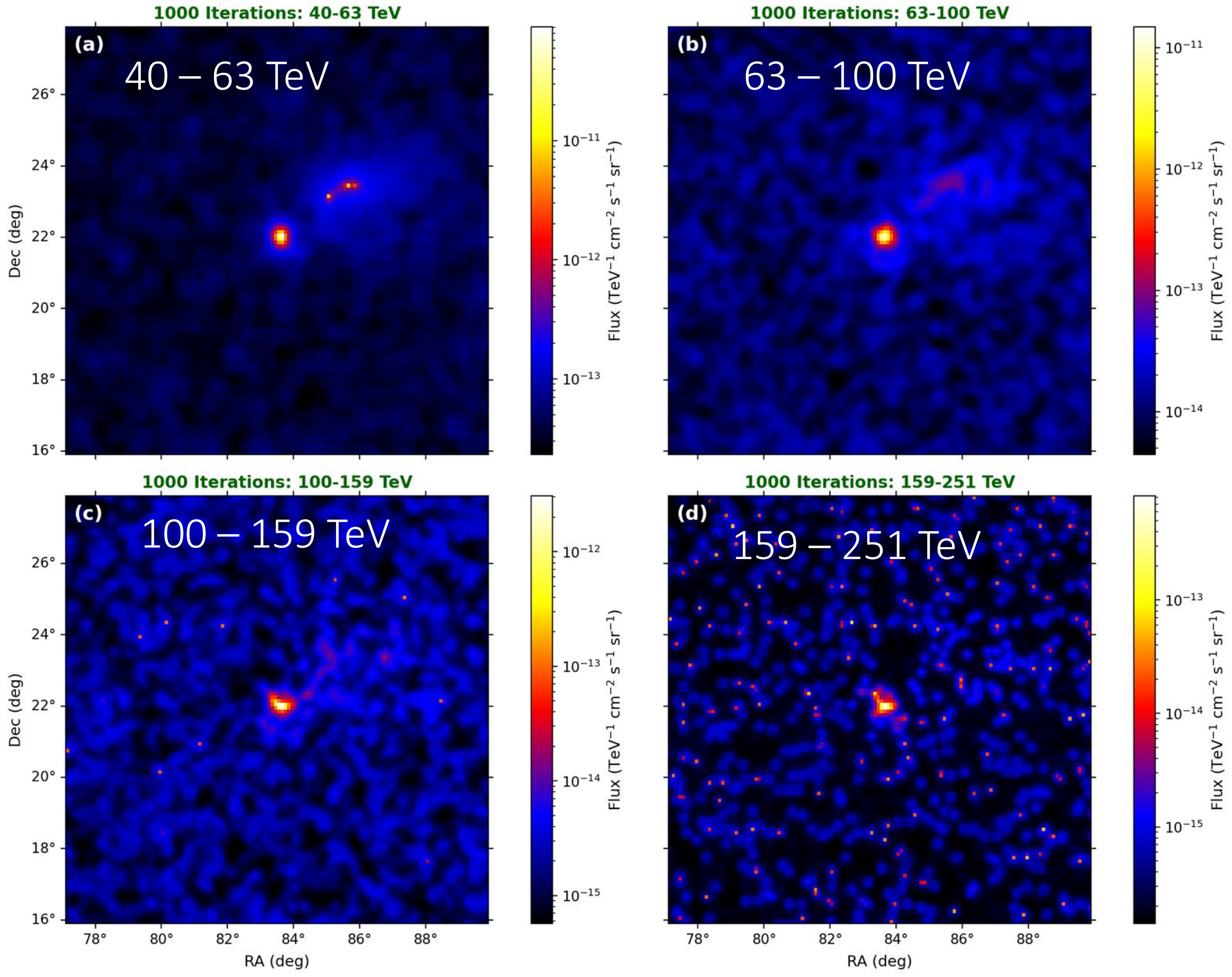

Angular Resolution Test

RL Radial Profiles vs. 0.1˚ Gaussian Model

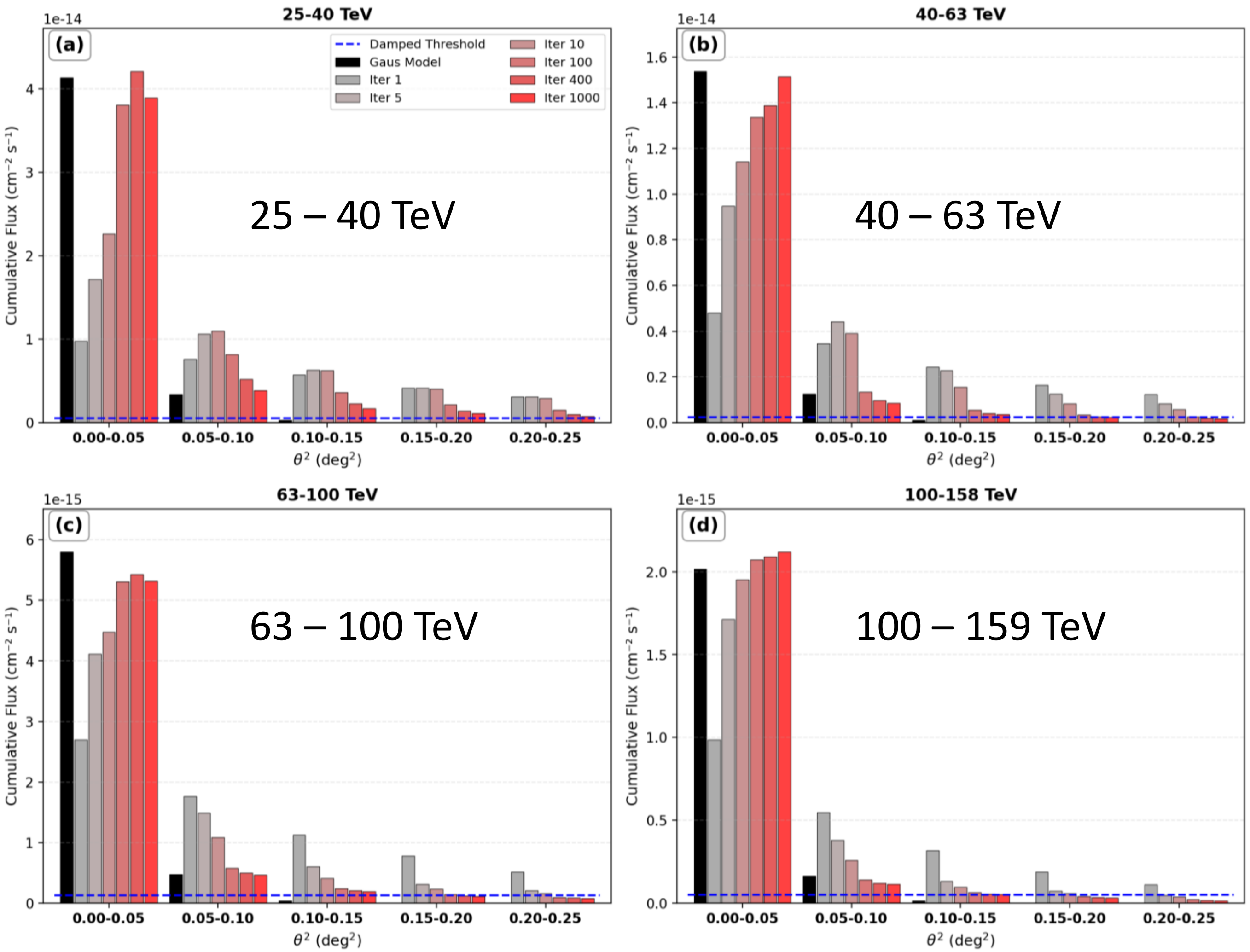

Damped RL recovers Crab radial flux distribution down to ~0.1deg resolution.

More example

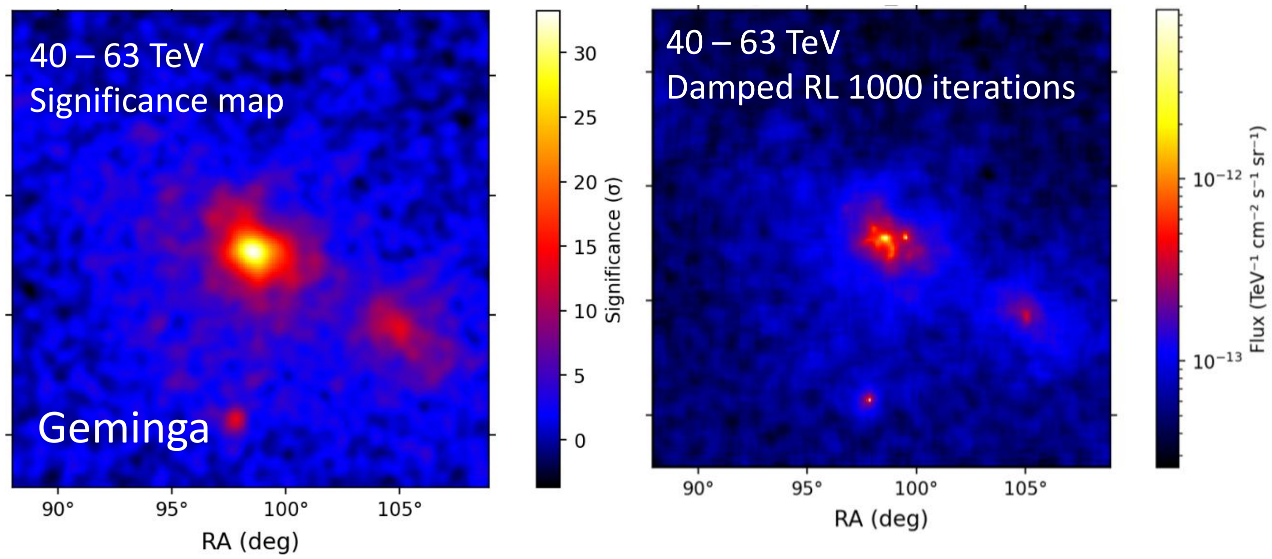

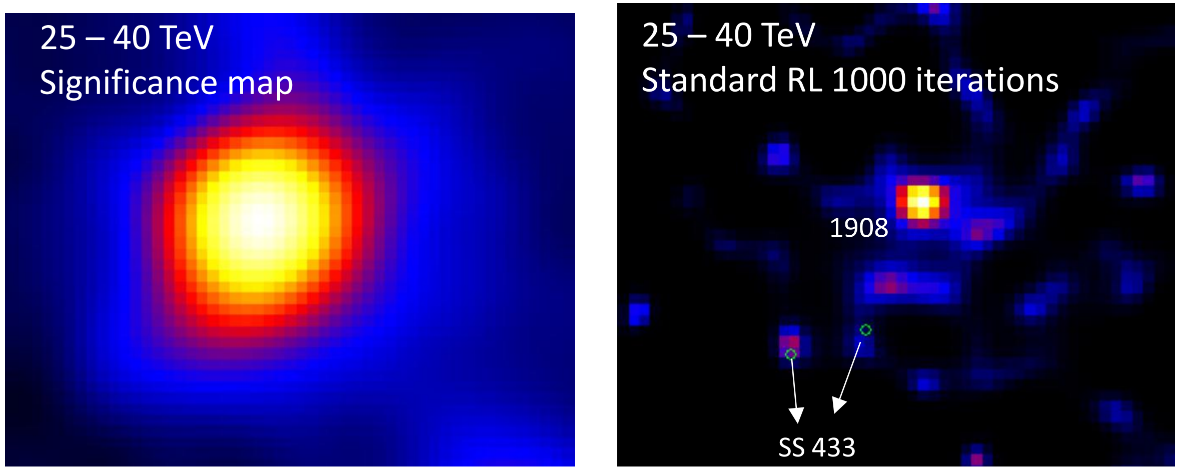

1 Provide better resolution than significance map.
2 Flux is more intuitive than significance.
3 Provide initial positions for 3D likelihood fitting in complex regions. And help searching for suitable gas templates.

However, RL cannot provide accurate statistical significance assessment; model-based likelihood fitting is therefore required to ultimately confirm the significance of the corresponding structures.

Multi-wavelength Context

Overview

- **Largest star-forming region** in the local spiral arm
- Hosts **Cygnus OB2** — hundreds of massive O/B stars
- Previous detections: Milagro, Fermi-LAT, ARGO-YBJ, VERITAS, HAWC
- LHAASO: **UHE gamma-ray bubble** extending to PeV energies

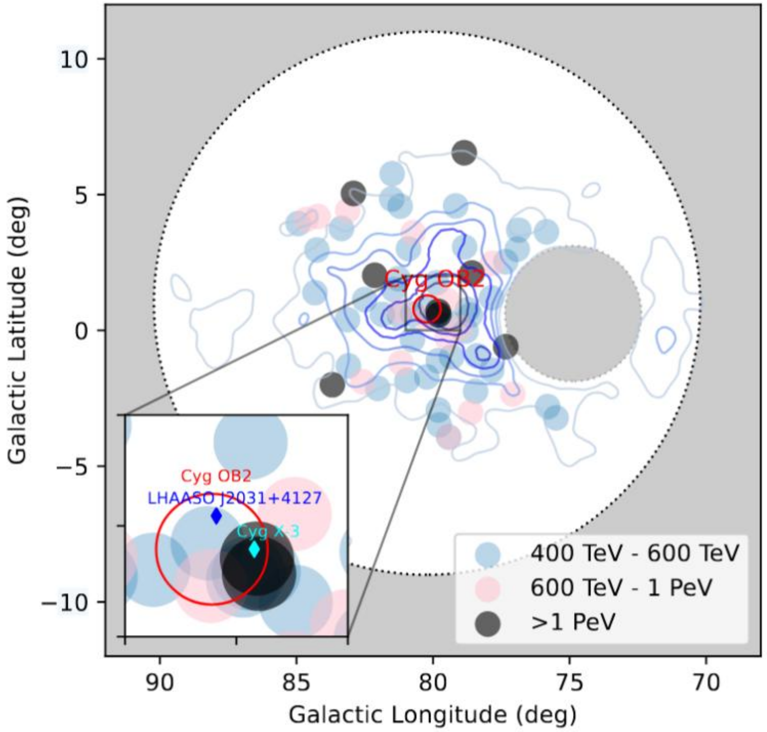

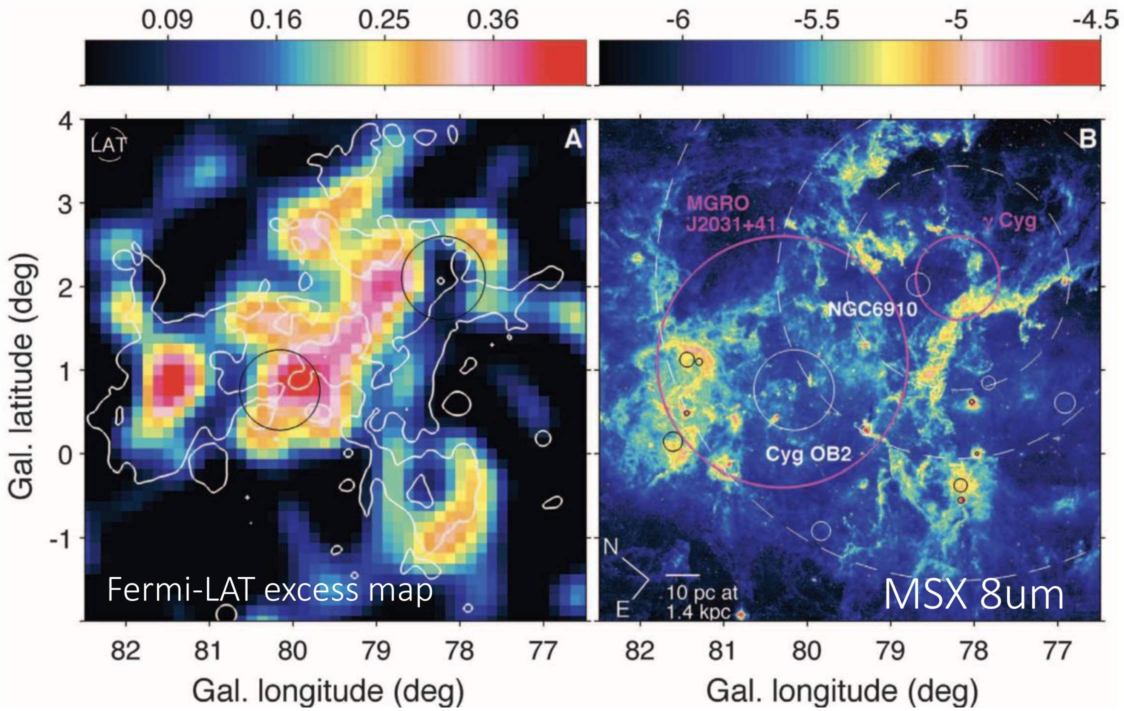

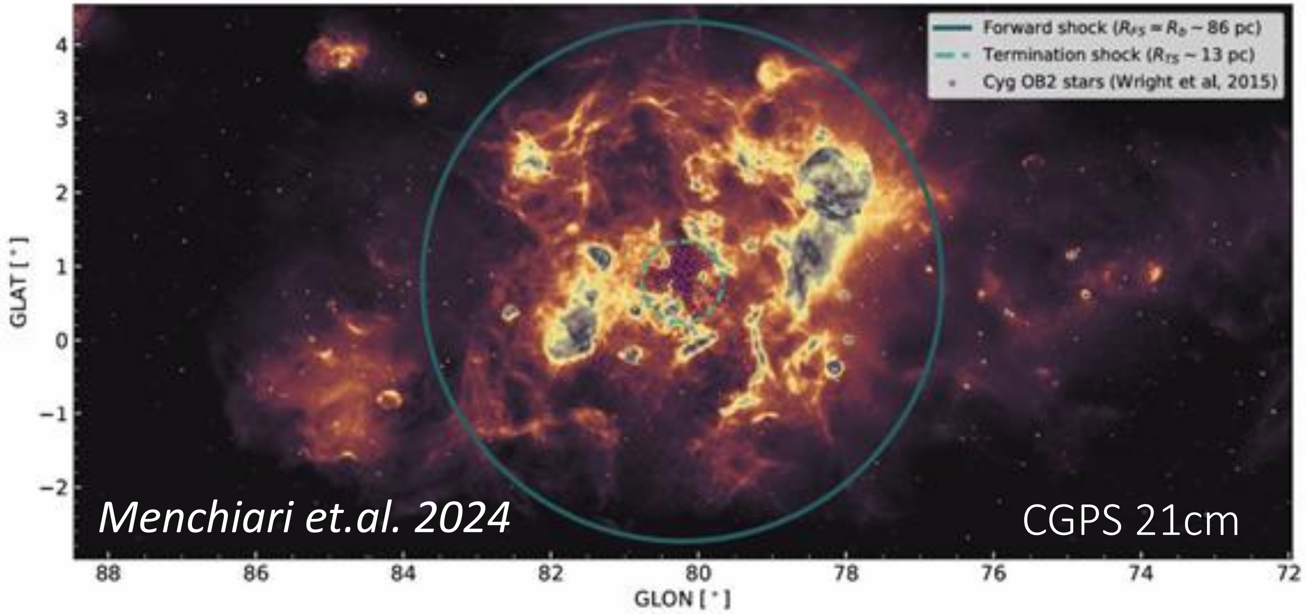

RL results

25 - 40 TeV

Data: all KM2A data to 20250731

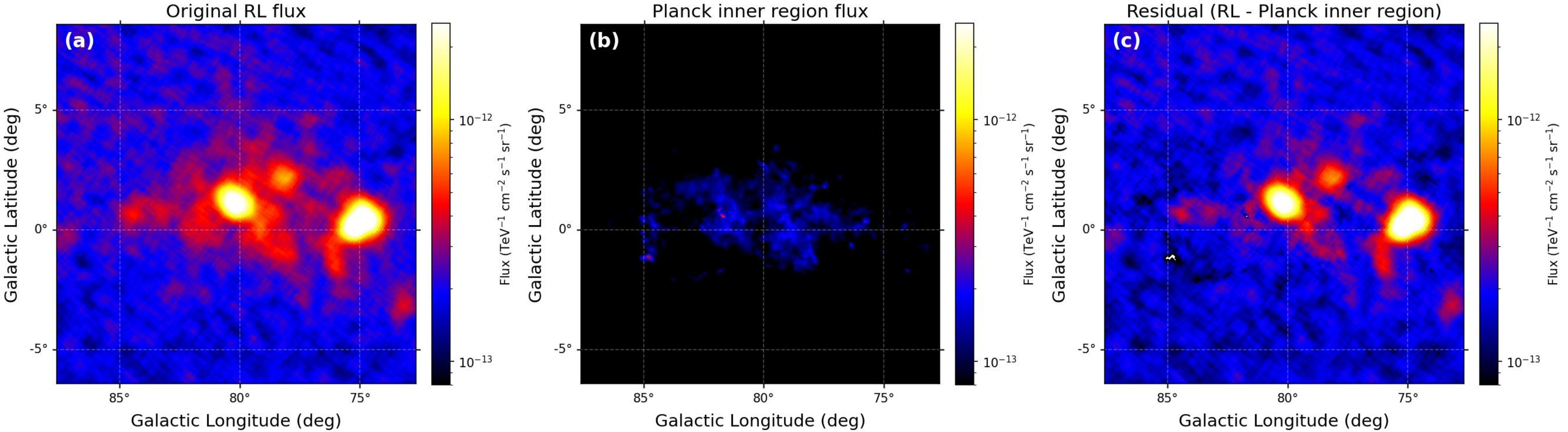

Cygnus X —Three Sub-regions

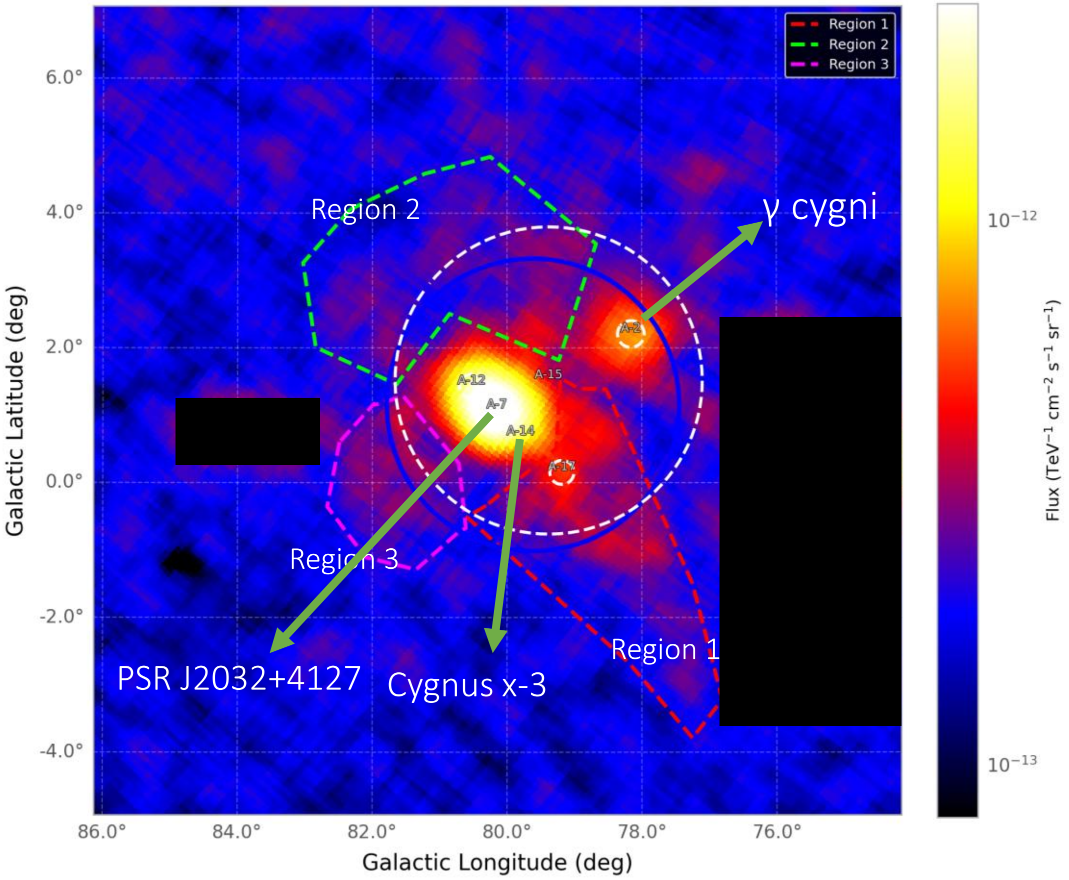

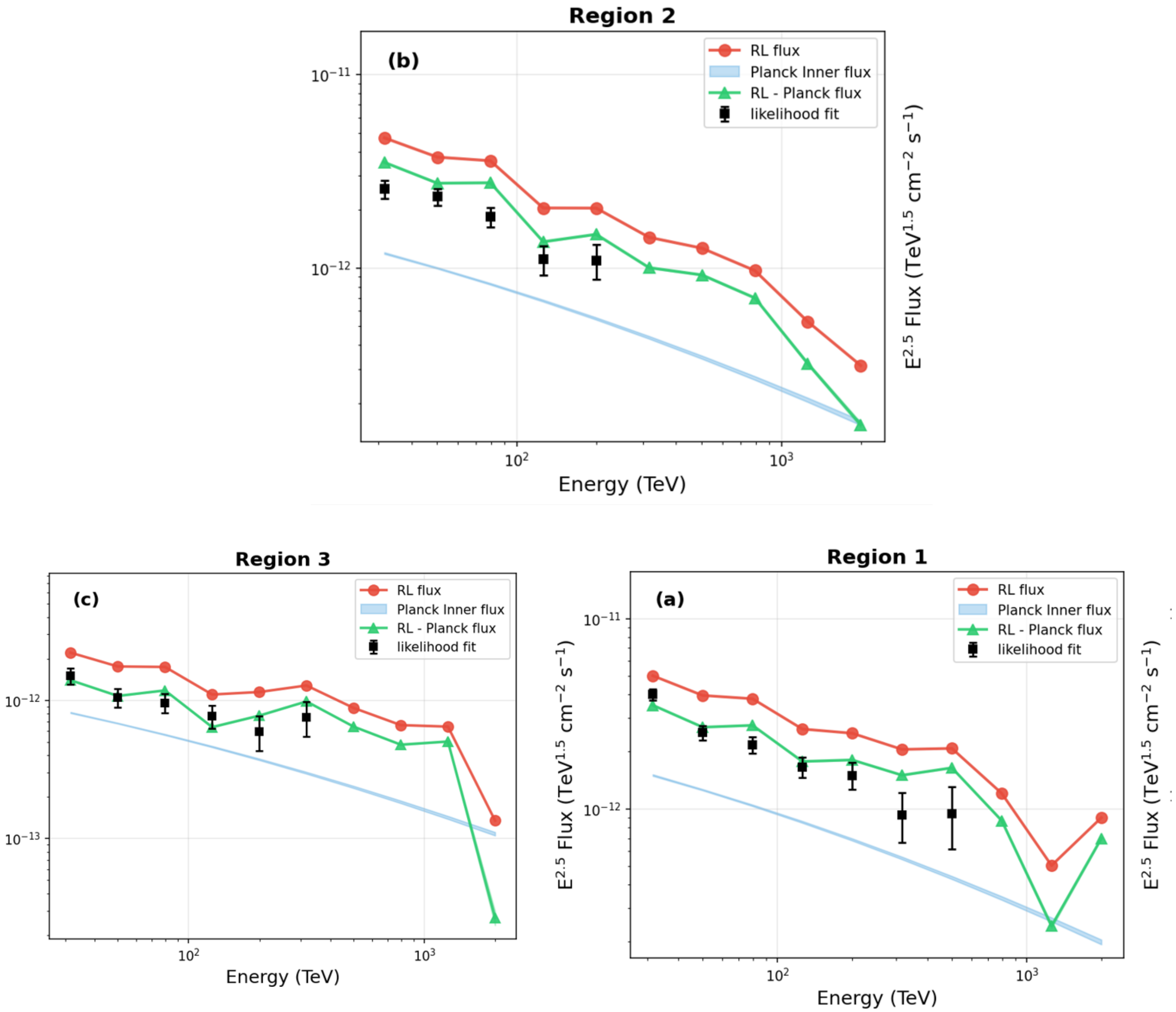

Blue: LHAASO Cygnus 2° extensive gaus source *(LHAASO 2024)*

White: Sources obtained through an iterative 3D likelihood fitting

Multi-wavelength comparison

Shell & cavity

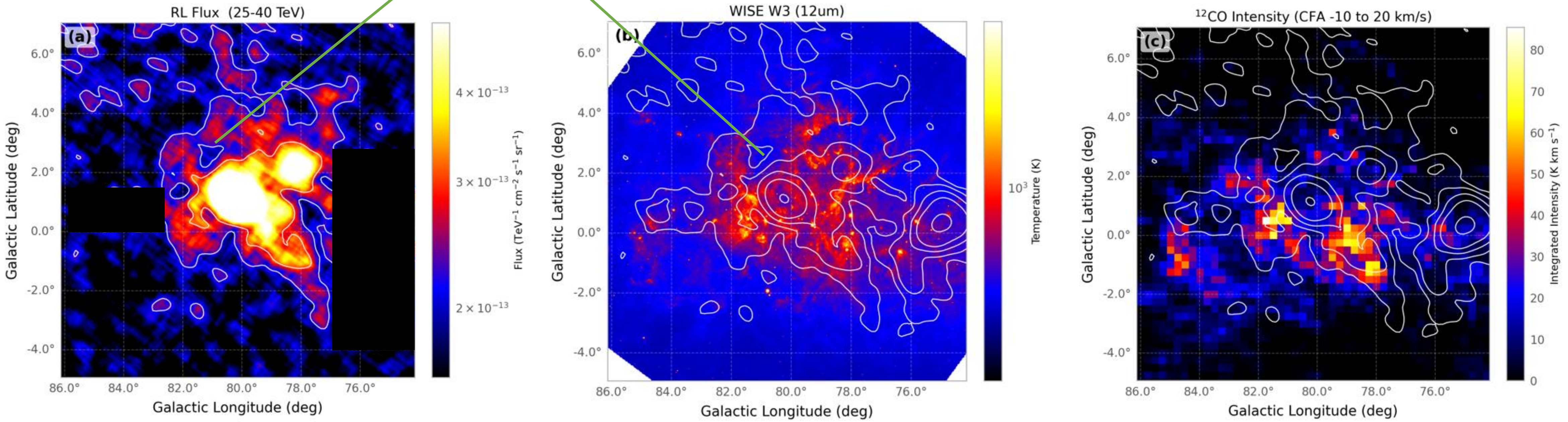

Multi-wavelength comparison

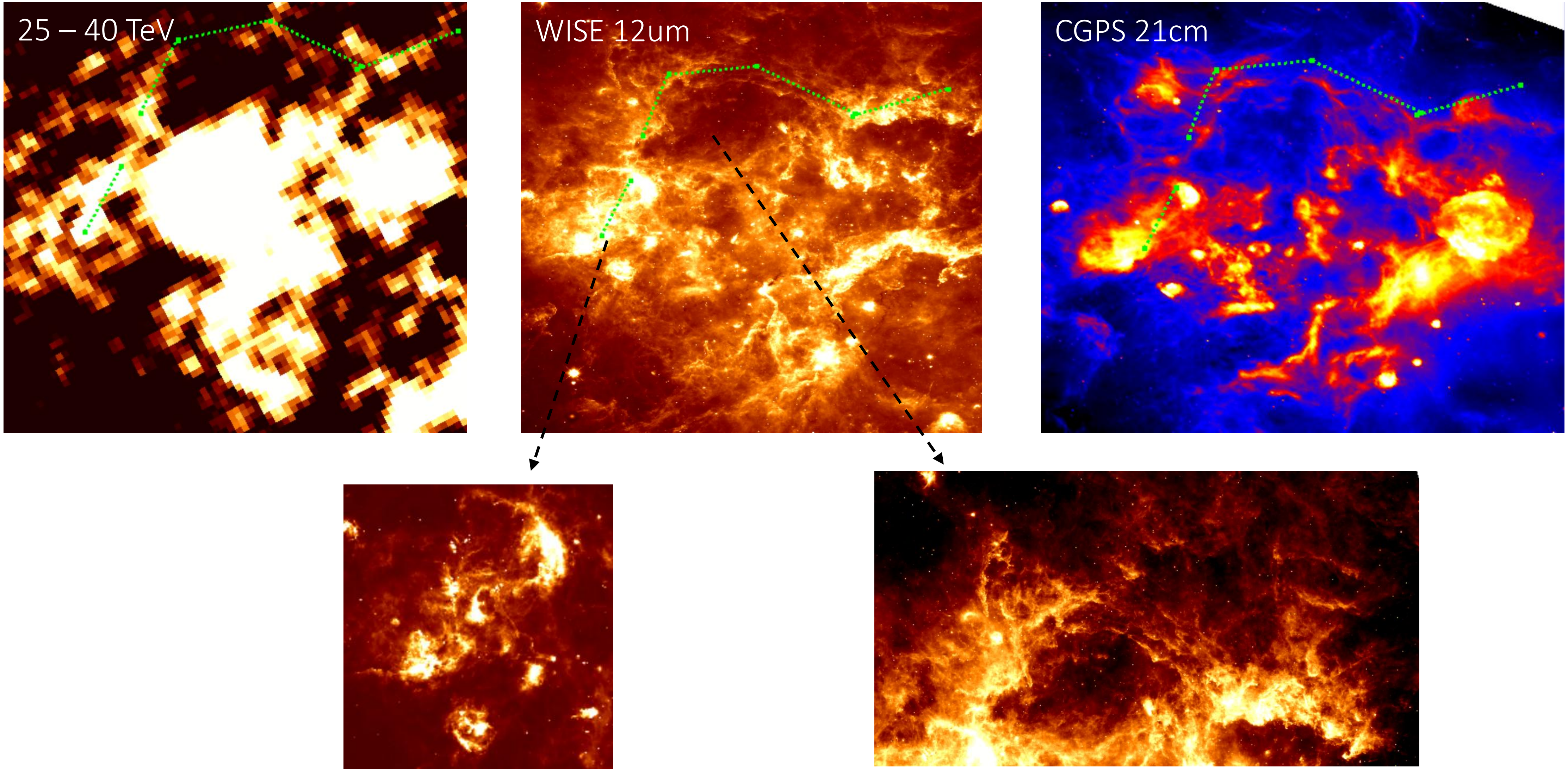

Possible scenario

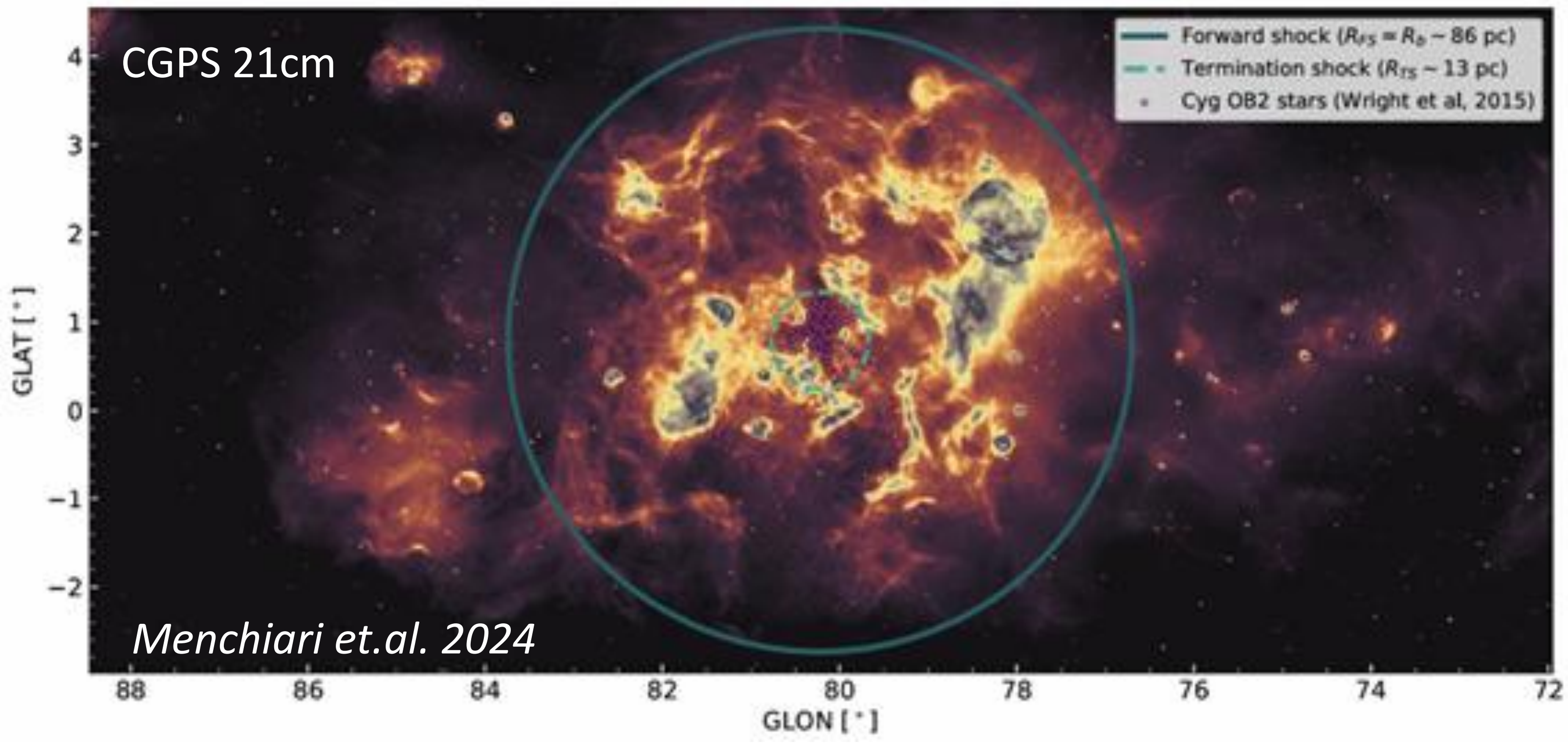

Cosmic rays accelerated inside Cygnus OB2 interact with the material accumulated at the forward shock of the super-bubble driven by Cygnus OB2

Implication

Hadronic Origin Evidence

Spatial correlation between TeV morphology and thermal dust emission (WISE 12 μm) supports hadronic origin

Link to Cygnus OB2

Shell & Cavity structure likely corresponds to photoionization edge around Cygnus OB2 or superbubble forward shock boundary

Outlooks

Measuring the distance of the shell & cavity structure, identify its relation with cygnus OB2

Get the significance of the shell & cavity structure, combining model-based likelihood fitting

Obtain the multi-wavelength spectral energy distribution of this region to test whether the Cygnus diffuse emission originates from the terminal shock produced by the Cygnus OB2 stellar wind, or alternatively from a supernova explosion

Summary

1. Application of RL deconvolution to LHAASO-KM2A cube data with position-energy-dependent response
2. Validated on Crab Nebula: ~0.1° resolution
3. Cygnus X: revealed TeV morphology with better resolution
4. Spatial correlation with hot dust suggests **hadronic origin**
5. Shell & Cavity near Cygnus OB2 suggests **superbubble connection**

Thank You!